

Possible transition between charge density wave and Weyl semimetal phase in $Y_2Ir_2O_7$ Abhishek Juyal,^{1,2,3,*} Vinod Kumar Dwivedi^{4,5,*} Sonu Verma,^{1,6} Shibabrata Nandi^{6,7,8} Amit Agarwal,^{1,†} and Soumik Mukhopadhyay^{1,‡}¹*Department of Physics, Indian Institute of Technology Kanpur, Kanpur 208016, India*²*Georgia Tech Lorraine, IRL 2958-CNRS, 57070 Metz, France*³*School of Physics, Georgia Institute of Technology, Atlanta, Georgia 30332, USA*⁴*Materials Science Program, Indian Institute of Technology Kanpur, Kanpur 208016, India*⁵*Department of Physics, Indian Institute of Science, Bengaluru 560012, India*⁶*Center of Theoretical Physics of Complex Systems, Institute for Basic Science (IBS), Daejeon 34126, Republic of Korea*⁷*Forschungszentrum Jülich GmbH, Jülich Centre for Neutron Science (JCNS-2)**and Peter Grünberg Institut (PGI-4), JARA-FIT, 52425 Jülich, Germany*⁸*RWTH Aachen, Lehrstuhl für Experimentalphysik IVc, Jülich-Aachen Research Alliance (JARA-FIT), 52074 Aachen, Germany*

(Received 1 June 2022; revised 17 August 2022; accepted 6 October 2022; published 26 October 2022)

The subtle interplay of band topology and symmetry broken phase, induced by electron correlations, has immense contemporary relevance and potentially offers novel physical insights. Here, we provide evidence of possible charge density wave (CDW) in bulk $Y_2Ir_2O_7$ for $T < 10$ K, and the Weyl semimetal (WSM) phase at higher temperatures. We observe the following characteristic properties of the CDW phase: (i) current induced nonlinear conductivity with negative differential resistance at low temperature, (ii) low-frequency Debye-like dielectric relaxation at low temperature with a large dielectric constant $\sim 10^8$, and (iii) an anomaly in the temperature dependence of the thermal expansion coefficient. The WSM phase at higher temperature is analyzed using the dc and ac transport measurements, which show an inductive response at low frequencies. More interestingly, we show that by reducing the crystallite size, the low-temperature CDW phase can be eliminated leading to the restoration of the WSM phase.

DOI: [10.1103/PhysRevB.106.155149](https://doi.org/10.1103/PhysRevB.106.155149)**I. INTRODUCTION**

Strong electron-electron correlation and topology are generally considered mutually exclusive domains of physics. However, recent observations of interaction-driven topological phase transition [1,2] have opened up prospects for exploring the interplay of correlation and topology. In fact, Weyl semimetals (WSM) were first predicted in correlated pyrochlore iridates, $R_2Ir_2O_7$ ($R = Y, Eu, Nd$) [3]. These $5d$ orbital-based iridates can host a variety of topological and quantum phases in addition to the WSM phase [3–13]. The search for Fermi arc surface states in $Y_2Ir_2O_7$ and other iridates has been unsuccessful due to the unavailability of good quality single crystals and inadequate surface preparation rendering techniques such as ARPES and STM ineffective. However, there could be a more fundamental reason: Weyl nodes could gap out forming density wave instabilities due to chiral symmetry breaking induced by Coulomb interaction [14–16]. Recently, a large negative contribution to the longitudinal magnetoresistance in the sliding mode of the charge density wave (CDW) phase of WSM candidates including nanorods based on $Y_2Ir_2O_7$ have been observed [15,17]. The negative

longitudinal magnetoresistance in such cases originates from the axionic contribution of the chiral anomaly to the phason current [15,17].

Apart from $Y_2Ir_2O_7$, among the iridates family, $Nd_2Ir_2O_7$ shows a quadratic band touching at the Γ point, which gaps out at low temperature [18]. The claim of metal-semimetal transition in the optical conductivity data for $Eu_2Ir_2O_7$ [19] needs to be backed by other more compelling evidence. Epitaxial strain-induced all-in, all-out ordering in thin films of $Pr_2Ir_2O_7$ breaks the time-reversal symmetry, possibly leading to WSM phase [20]. Although single crystalline nanorods of $Y_2Ir_2O_7$ have shown evidence of possible chiral anomaly in the gapped out WSM phase [14,15], the question remains whether the conclusions drawn can be extended to bulk $Y_2Ir_2O_7$ as well.

Here, we present experimental evidence of gapped out WSM ground state in bulk $Y_2Ir_2O_7$, showing characteristics of (axionic) CDW with a possible transition to WSM phase above 10 K. Both the CDW phase in bulk $Y_2Ir_2O_7$ for $T < 10$ K, and the WSM phase above $T > 10$ K are characterized independently via dc and ac transport measurements. The possibility of a WSM to CDW transition is also supported by our thermal expansion experiments. The CDW gap opening can be prevented by reducing the grain size, thus extending the WSM state to low (~ 1 K) temperatures. Remarkably, we find the dc transport in nanocrystalline samples to be consistent

*These authors contributed equally to this work.

†amitag@iitk.ac.in‡soumikm@iitk.ac.in

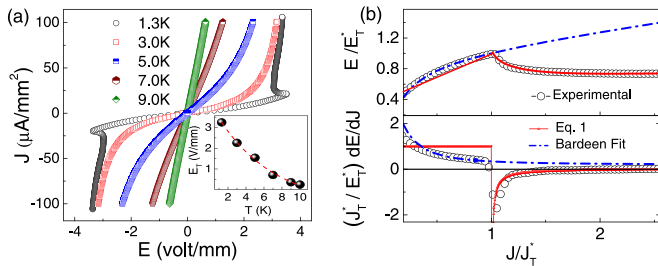


FIG. 1. CDW phase in $\text{Y}_2\text{Ir}_2\text{O}_7$ for $T < 10$ K. (a) dc IV characteristics for bulk $\text{Y}_2\text{Ir}_2\text{O}_7$ showing CDW depinning induced nonlinear transport below 9 K, and S-shaped negative differential resistance at 1.3 K. The inset shows depinning threshold (E_T) for positive bias, which follows $E_T \propto \exp[-T/T_0]$, with $T_0 \approx 3$ K. (b) Characteristic plot (at $T = 1.3$ K) of E (top) and dE/dJ (bottom) normalized to E_T and J_T where current is regulated. The continuous lines are the theoretical fits to Bardeen's tunneling theory in pinned CDW for $J \in [J_T, J_T^*]$ and to Eq. (1) for $J > J_T^*$ in the depinned regime.

with the Coulomb interaction-induced diffusive transport in the WSM phase [21].

II. EXPERIMENTAL RESULTS AND DISCUSSION

Electrical transport measurements were performed on bulk polycrystalline sample of grain size more than 200 nm and nanocrystalline samples (of average crystallite size of 50 and 40 nms, as calculated from the line broadening in the XRD spectra and further confirmed by TEM measurements). See Supplemental Material (SM) [22] for details of sample preparation and characterization. To start with, we present the evidence for the CDW phase in the bulk sample, which is observed in current-driven nonlinear IV characteristics shown in Fig. 1. The linear conductivity at low voltage is followed by the onset of nonlinear conduction at higher voltages when the CDW starts sliding. More interestingly, the nonohmic IV characteristics at 1.3 K also exhibits current controlled negative differential resistance (NDR). Both of these effects are associated with CDW depinning, and the resultant constant current IV characteristic showing NDR is commonly referred to as S-shaped response. The NDR is not observed at higher temperatures although the nonlinear IV characteristic is found to persist up to 9 K in Fig. 1(a).

The essential features of these measurements are captured by a simple model describing the dynamics of the CDW phase. The CDW phase may be weakly pinned by impurities, lattice defects, or confined by the grain boundaries [23]. Electrical transport occurs due to the translational motion of the CDW and that of the normal carriers. At low electric field (or current) values below a critical threshold, $E < E_T$ (or $J < J_T$), normal quasiparticles carry the current leading to ohmic behavior while the CDW domains remain pinned. For $E > E_T$ (or $J > J_T$), the CDW domains become partially depinned, leading to nonlinear contribution to conductivity. In this regime, the transport is described by Bardeen's CDW tunneling theory [24]. The threshold field directly probes the effectiveness of the pinning of the CDW order parameter. We find $E_T(T) = E_0 \exp(-T/T_0)$, with $T_0 \approx 3$ K denoting the

strength of the pinning potential [25], as shown in the inset of Fig. 1(a).

On increasing the current (or field) beyond a second threshold, $J > J_T^*$ (or $E > E_T^*$), the CDW dislodges and moves with a single phase. Consequently, for $J > J_T^*$ the voltage across the sample drops abruptly as the current increases. This leads to NDR as shown in Fig. 1(a) for $T = 1.3$ K. In this regime, the conductivity is dominated by coherent CDW transport, which is well described by the damped dynamics of the CDW phase [26,27]. In a constant current experiment, the nonlinear I-V characteristics above the depinning threshold E_T^* is given by [26,28]

$$E = \frac{J}{\sigma_n} - \frac{\beta E_T^*}{1 + \beta} \left[\left(\frac{J}{J_T^*} \right)^2 - 1 \right]^{1/2}. \quad (1)$$

Here σ_n is the ohmic conductivity of the normal quasiparticles, and β is a system- and temperature-dependent parameter. The conductivity dE/dJ has a discontinuity at the NDR threshold J_T^* . This discontinuity is explicitly shown for the $T = 1.3$ K curve in both panels of Fig. 1(b), along with the corresponding fit to Bardeen's tunneling theory for $J_T < J < J_T^*$ and to Eq. (1) for $J > J_T^*$. This is a demonstration of the coexistence of quantum and classical regime of the CDW transport. Interestingly, the IV characteristics in the NDR regime also show negative (positive) longitudinal (transverse) magnetoresistance (MR), similar to that found in single crystalline nanorods of $\text{Y}_2\text{Ir}_2\text{O}_7$ [15]. This is shown explicitly in Fig. S3 in SM [22]. The response of the I-V characteristics in the longitudinal and transverse geometry to the magnetic field leading to negative and positive MR, respectively, suggests that joule heating can be ruled out as a possible origin of the NDR. However, the observation of NDR may not conclusively prove the existence of CDW order. We now provide additional evidence to support our claim.

We measure the low-frequency dielectric response using the standard lock-in technique. For $T < 10$ K, the ac transport measurements show distinctly different behavior compared to the measurements at higher temperatures, as highlighted in Fig. 2. In particular, we find that for $T < 10$ K, the dielectric constant shows a Debye-like relaxation indicating a CDW phase. Similar to the observations in single crystalline $\text{Y}_2\text{Ir}_2\text{O}_7$ nanorods [14,15], we find that the dc conductivity and the peak frequency (ω_p) of the imaginary part of the dielectric constant show an Arrhenius-like temperature dependence: $\sigma_0 \propto \omega_p \propto \exp[-\Delta/T]$, with $\Delta = 16.1$ K. Physically this occurs due to the screening of the damped collective charge oscillations of the CDW by the thermally excited normal carriers [29,30]. This gives us a mean-field estimation of the CDW transition temperature ($2\Delta = 3.52 T_{\text{CDW}}$) to be $T_{\text{CDW}} \approx 9.15$ K, consistent with the dc measurements. The corresponding coherence length can be estimated to be $\xi_0 \approx 2.4$ nm, which is much smaller than the grain ~ 1 μm , and similar to the observed value in other polycrystalline samples [31].

For $T > 10$ K, the real component of the conductivity [see Fig. 2(a)] displays behavior similar to that of the Weyl semimetal phase with short-range disorder [21] [see inset in Fig. 2(a)]. The conductivity remains almost constant for very low frequencies ($\omega < 10^2$ Hz), decreases for intermediate fre-

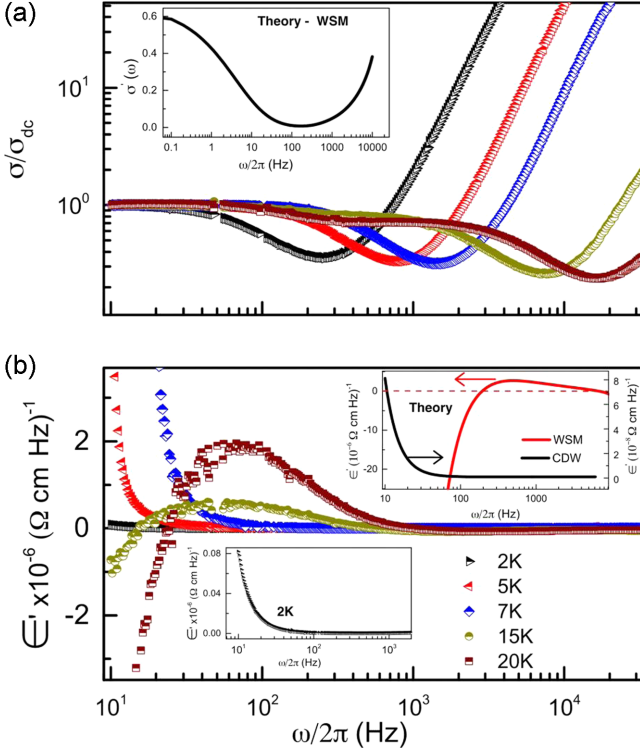


FIG. 2. (a) $\text{Re}[\sigma(\omega)]t$ for the bulk polycrystalline samples shows a WSM-like behavior for $T > 10$ K, while for $T < 10$ K it shows a CDW behavior with Debye-like relaxation. The inset shows the theoretically calculated conductivity for disordered WSM. (b) The real part of dielectric function for $T < 10$ K is consistent with Debye relaxation (see black curve in the top inset). The bottom inset shows the blown-up portion of the experimental plot at 2 K. In contrast, the WSM state for $T > 10$ K shows a crossover from negative to positive dielectric constant, consistent with the theoretical results for WSM, shown by the red curve in the top inset.

quencies ($\omega \in [10^2, 10^3]$ Hz), and then increases very rapidly for $\omega \approx 5 \times 10^4$ Hz, depending on the temperature. Within the Born approximation, the conductivity in WSM with dilute and random short-range disorder is given by [21]

$$\sigma(\omega, T) = \frac{e^2 v_F^2}{h\gamma} J\left(\frac{N\omega}{\omega_0}, \frac{NT}{\omega_0}\right). \quad (2)$$

Here, $\omega_0 = 2\pi v_F^3/\gamma$ is the characteristic frequency set by the disorder scale γ , and N denotes the number of Weyl nodes. In Eq. (2), we have defined $J(\bar{\omega}, \bar{T}) = \frac{4}{3} \int \frac{d\bar{\epsilon}}{2\pi} \frac{[f_{\bar{T}}(\bar{\epsilon}) - f_{\bar{T}}(\bar{\epsilon} + \bar{\omega})]}{\omega} I(\bar{\epsilon} + \bar{\omega}, \bar{\epsilon})$, with $\bar{x} = x/\omega_0$, $f_{\bar{T}}(\bar{\omega}) = (1 + e^{\bar{\omega}/\bar{T}})^{-1}$ is the Fermi function. The explicit form of the function $I(\bar{\epsilon} + \bar{\omega}, \bar{\epsilon})$ is given in the SM [22]. Equation (2) implies that $\sigma(\omega)$ diverges as $\omega \rightarrow \omega_0$, signaling a breakdown of the Born approximation [21]. Thus, we estimate that $\omega_0 \approx 4\pi \times 10^4$ rad/s, for the $T = 20$ K curve in Fig. 2. In the $\omega \ll T$ limit (valid for our experiments), Eq. (2) leads to $\sigma(\omega \rightarrow 0) \approx 2e^2\omega_0/(3\hbar v_F)$. Using the estimated value of ω_0 , we calculate $\sigma(\omega \rightarrow 0) = 5.2 \times 10^{-5}/(\Omega \text{ cm})$, which is reasonably close to the measured value of $\sigma(\omega \rightarrow 0) = 3.2 \times 10^{-5}/(\Omega \text{ cm})$. This nonmonotonic behavior in the low-frequency conductivity for $T > 10$ K is also accompanied by a nonmonotonic

behavior in the dielectric constant, as shown in Fig. 2(b). The real part of the dielectric constant is negative for low frequencies, it increases to become positive at intermediate frequencies, and then decreases again to settle just below the zero axis, consistent with the theoretical calculation shown in the inset of Fig. 2(b). In the CDW regime for $T < 10$ K, the dielectric function shows a monotonically decreasing behavior with frequency, similar to that seen in other CDW systems, including crystalline nanorods of $\text{Y}_2\text{Ir}_2\text{O}_7$ [14, 15]. Remarkably, the CDW transition temperature in $\text{Y}_2\text{Ir}_2\text{O}_7$ drops from $T_{\text{CDW}} > 300$ K in single crystalline nanorods [15] to around 10 K in bulk polycrystalline samples.

The suggestion of CDW to WSM transition in $\text{Y}_2\text{Ir}_2\text{O}_7$ can also be seen from the temperature dependence of the dc conductivity. To distinguish the nature of dc transport between activated and power-law behavior, we plot $-\rho^{-1} \frac{d\rho}{dT}$ as a function of T on a log-log scale for bulk sample in Fig. 3(a). The activated behavior of the dc transport for $T < 10$ K (with a slope ≈ -2 in the CDW phase) and a power-law behavior above $T > 10$ K (with a slope ≈ -1 in the WSM phase) is clearly established. The CDW transition temperature estimated by fitting the activated dc transport [$\rho \propto e^{\Delta_{\text{CDW}}/(k_B T)}$] below $T < 10$ K is consistent with the earlier estimated value.

For $T > 10$ K, a clear power-law behavior in the resistivity, $\rho(T) \propto T^{-n}$, is found till $T \approx 80$ K. However, different experiments have reported varying power laws for the resistivity of $\text{Y}_2\text{Ir}_2\text{O}_7$. While our bulk samples show $n = 3.02$, close to the value of $n = 3.1$ reported in Ref. [32], there have also been reports of $n = 4.3$ [33], $n = 4.6$ [34], and $n = 4.8$ [35]. See Fig. 3(b) for a comparison, where we estimate the exponents by digitizing and fitting all the available data sets up to 50 K, for uniformity. This clearly shows that the low-temperature power-law behavior of $\rho(T)$ in $\text{Y}_2\text{Ir}_2\text{O}_7$ is nonuniversal, and possibly dependent on various factors such as crystallite size, disorder layout, etc.

The nanocrystalline samples show a power-law exponent close to unity, which has also been predicted to arise in the Coulomb interaction dominated diffusive transport regime of WSM. The predicted dc conductivity [21] is given by

$$\sigma_{\text{dc}}(T) = \frac{e^2}{h} \frac{k_B T}{\hbar v_F(T)} \frac{0.45}{\alpha_T^2 \ln \alpha_T^{-1}}. \quad (3)$$

Here, the renormalized fine structure constant is $\alpha_T = \alpha_1 [1 + \frac{(N+2)\alpha_1}{3\pi} \ln \frac{(\hbar\Lambda)}{k_B T}]$, and the renormalized Fermi velocity is $v_F(T) = v_F (\alpha_1/\alpha_T)^{2+2/N}$. The number of Weyl nodes is specified by $N = 24$, and Λ is a momentum cutoff set by the separation between the Weyl nodes. This model description for $\rho(T)$ [21] fits our experimental data for the nanocrystalline sample, remarkably well over the entire temperature range, as shown in Fig. 3(c).

This naturally prompts the question: Why does the CDW gap close on reducing the particle size (or increasing the surface to volume ratio), leading to the restoration of the WSM phase in $\text{Y}_2\text{Ir}_2\text{O}_7$ [36]? The possibility of the quantum confinement gap [$\Delta_{\text{QC}} \approx \hbar^2/(m_e L^2)$] becoming larger than the CDW gap is unlikely in this case as, even for an average particle size of 50 nm we have $\Delta_{\text{QC}} \sim 0.03$ meV, which is almost 30 times smaller than $k_B T_{\text{CDW}} \approx 0.86$ meV. We rule out the possibility of the softening of phonon mode due to

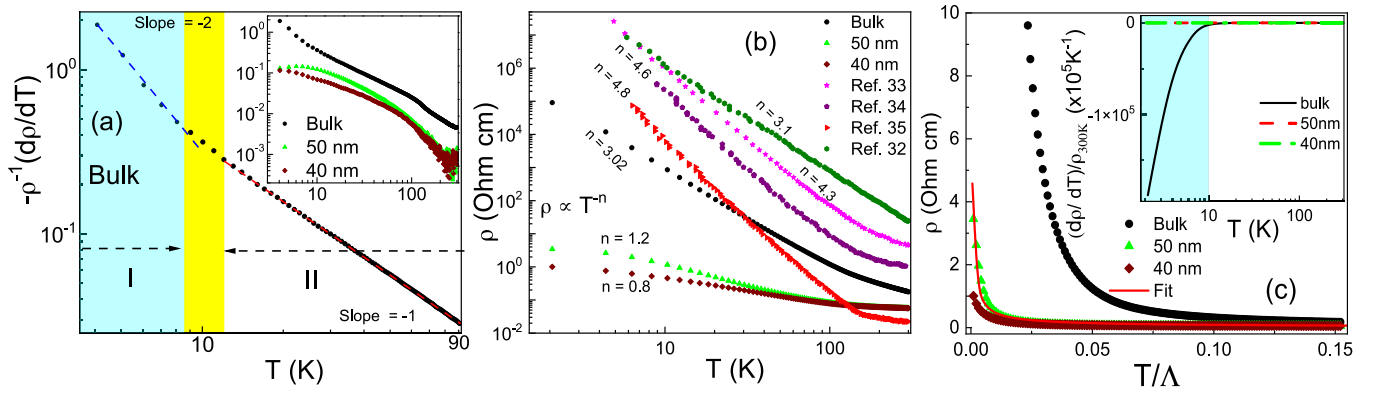


FIG. 3. $\rho(T)$ of bulk polycrystalline sample. (a) $\rho^{-1} \frac{d\rho}{dT}$ plotted as a function of T clearly shows an activated behavior (with slope ≈ -2) for $T < 10$ K and a power law (with slope ≈ -1) above $T > 10$ K. The inset shows the same plot for the bulk and nanocrystalline samples together over the entire temperature range. (b) Comparison of the power-law exponents from different experiments with that for our bulk, and nanocrystalline samples. (c) The variation of the dc conductivity of bulk and the nanocrystalline (average particle size of 40 nm and 50 nm) samples with temperature, compared with the Coulomb interaction-induced diffusive transport model (continuous line) for interacting WSM. Inset: Plot of $\frac{d\rho}{dT}$ vs T clearly shows the resistive anomaly around T_{CDW} for the bulk sample.

increased surface contribution by our specific heat measurements (not shown here), which shows an enhancement in the θ_D in the nanocrystalline sample ($\theta_D = 503.9 \pm 14.5$ K) compared to the corresponding bulk value ($\theta_D = 462.6 \pm 9.1$ K). One possibility supported by our x-ray spectroscopy data is the increase in carrier kinetic energy in nanocrystalline samples owing to the enhancement of the concentration of higher oxidation states, Ir^{5+} (see Fig. S2 in SM) or due to quantum confinement effects. The increased kinetic energy in nanocrystalline samples is likely to reduce the impact of correlation effects and reduce the T_{CDW} . Recently pressure-induced closing of a large CDW gap has been observed in $\text{Ta}_2\text{Se}_8\text{I}$, which exhibits a Weyl semimetal to CDW transition close to room temperature in ambient pressure [37]. In our case, the CDW gap being much smaller, increased surface pressure due to reduction of particle size could be effectively playing a similar role.

Heat capacity measurement is expected to show anomaly around the CDW transition. We have performed heat capacity measurements on the bulk sample (not shown in figure), which does not exhibit any anomaly around the transition temperature. This can possibly be due to the polycrystalline nature of the sample, which makes these measurements less sensitive to phase transitions. Thermal expansion measurements offer an alternative and highly sensitive way to detect phase transitions for CDW materials [38]. For independent confirmation of the CDW phase transition in $\text{Y}_2\text{Ir}_2\text{O}_7$, we performed thermal expansion measurements using a capacitive dilatometer having sub-Å resolution with high sensitivity of $\Delta L/L \sim 10^{-10}$ at low temperatures. We find that the changes in thermal expansion in $\text{Y}_2\text{Ir}_2\text{O}_7$ are very small but detectable, thanks to the extremely high resolution of the capacitive dilatometer. It also indicates that the corresponding changes in heat capacity would be very small and may remain undetectable particularly for polycrystalline samples (as of now, $\text{Y}_2\text{Ir}_2\text{O}_7$ is unavailable in single crystalline bulk form). We measured the linear thermal expansion coefficient, $\alpha(T) \equiv dL/dT$, and verified it for different heating and cooling rate. The relative thermal expansion $\Delta L/L$, shown in Fig. 4, decreases mono-

tonically with the lowering of temperature. However, there is an anomaly at $T \approx 10.4$ K (consistent with the estimated $T_{CDW} \approx 9.15$ K from transport measurements) with relative dilatation of about 1.02×10^{-6} , as shown in Figs. 4(a)–4(b). The anomaly is highlighted further in the thermal expansion coefficient, which shows a sharp minimum at the same temperature. The $\alpha(T)$ curve fits reasonably well to the Debye model at higher temperature (see SM [22] for details, including Ref. [39]). The deviation from the Debye T^3 law in $\alpha(T)$

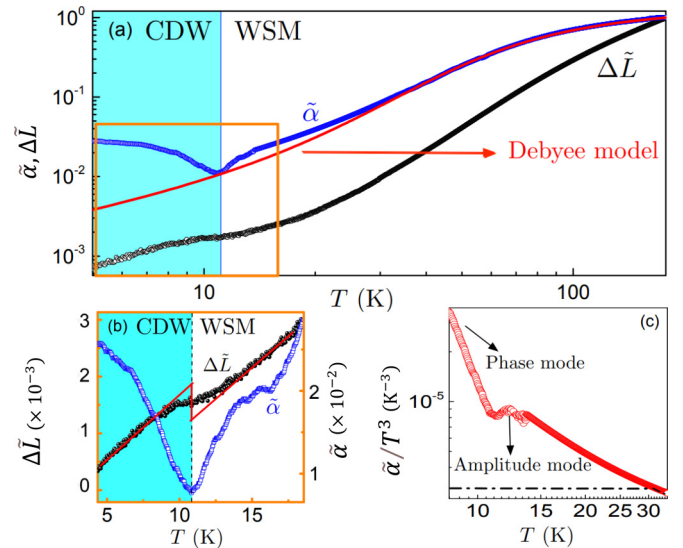


FIG. 4. (a) Variation of the relative length ($\Delta \tilde{L} = \Delta L / \Delta L_{T=180}$) and α ($\tilde{\alpha} = \alpha / \alpha_{T=180}$) with T for the bulk polycrystalline $\text{Y}_2\text{Ir}_2\text{O}_7$. The thermal expansion coefficient (blue curve) fits well with the Debye model (red curve) at high T . However, it shows an anomaly at low temperature coinciding with the T_{CDW} obtained from the transport measurements. This is highlighted in the zoomed panel (b) showing the low-temperature regime. Here, we have shifted the $\Delta \tilde{L}$ curve and the different linear fits below and above T_{CDW} are shown by red lines. (c) The deviation of α/T^3 from the Debye behavior (dashed black line) at low T .

is highlighted by plotting the residual $\alpha(T)/T^3$ vs T on the log-log scale in Fig. 4(c). Similar deviation from the T^3 law has also been observed in low-temperature specific heat for other CDW systems [40–42]. This deviation can be attributed to the splitting of the acoustic phonon mode (for $T < T_P$) into the gapped amplitude mode [which gives the hump for $T \sim T_P$ in $\alpha(T)/T^3$ plot in Fig. 4(c)] and the gapless phase mode [$T \rightarrow 0$ behavior of the $\alpha(T)/T^3$ curve] of the CDW condensate. Changes in thermal expansion in YIO are very small but detectable, thanks to the extremely high resolution of the capacitive dilatometer. It also indicates that corresponding changes in heat capacity would be very small and may be undetectable in bulk YIO. We have confirmed our thermal expansion data over several measurement cycles.

III. CONCLUSION

To summarize, we present experimental evidence of possible temperature and grain-size-dependent phase transition from the CDW phase to the WSM phase in bulk $\text{Y}_2\text{Ir}_2\text{O}_7$

using dc and ac transport experiments. The indirect evidence of phase transition is independently supported via thermal expansion measurements as well. The low-frequency dielectric response in the WSM phase at high temperature is consistent with the theoretically predicted response in WSM having short-range neutral disorder. Further, we provide evidence that the CDW gap is suppressed significantly on reducing crystallite size. The observed dc conductivity over a wide temperature range in the nanocrystalline $\text{Y}_2\text{Ir}_2\text{O}_7$ is consistent with the interaction-induced diffusive behavior characteristic of WSM. The grain-size-dependent tunability of the phase transition suggests the possibility of existence of a quantum critical point separating the WSM phase and the broken symmetry (possibly axionic) CDW phase.

ACKNOWLEDGMENTS

We acknowledge the Department of Science and Technology (DST) for project DST/NM/TUE/QM-6/2019(G)-IIT Kanpur and the Science and Engineering Research Board (SERB), for project MTR/2019/001520, of the Government of India, for financial support.

-
- [1] W. Shi, B. J. Wieder, H. L. Meyerheim, Y. Sun, Y. Zhang, Y. Li, L. Shen, Y. Qi, L. Yang, J. Jena, P. Werner, K. Koepf, S. Parkin, Y. Chen, C. Felser, B. A. Bernevig, and Z. Wang, *Nature Phys.* **17**, 381 (2021).
- [2] H. Polshyn, Y. Zhang, M. A. Kumar, T. Soejima, P. Ledwith, K. Watanabe, T. Taniguchi, A. Vishwanath, M. P. Zaletel, and A. F. Young, *Nature Phys.* **18**, 42 (2022).
- [3] X. Wan, A. M. Turner, A. Vishwanath, and S. Y. Savrasov, *Phys. Rev. B* **83**, 205101 (2011).
- [4] B. J. Kim *et al.*, *Phys. Rev. Lett.* **101**, 076402 (2008).
- [5] D. Pesin and L. Balents, *Nature Phys.* **6**, 376 (2010).
- [6] M. Kargarian, J. Wen, and G. A. Fiete, *Phys. Rev. B* **83**, 165112 (2011).
- [7] Y. Machida, S. Nakatsuji, S. Onoda, T. Tayama, and T. Sakakibara, *Nature (London)* **463**, 210 (2010).
- [8] K. Y. Yang, Y. M. Lu, and Y. Ran, *Phys. Rev. B* **84**, 075129 (2011).
- [9] W. Witczak-Krempa, G. Chen, Y. B. Kim, and L. Balents, *Annu. Rev. Condens. Matter Phys.* **5**, 57 (2014).
- [10] R. S. Singh, V. R. R. Medicherla, K. Maiti, and E. V. Sampathkumaran, *Phys. Rev. B* **77**, 201102(R) (2008).
- [11] V. K. Dwivedi, A. Juyal, and S. Mukhopadhyay, *Mater. Res. Express* **3**, 115020 (2016).
- [12] B. Ghosh and S. Mukhopadhyay, *Phys. Rev. B* **103**, 165135 (2021).
- [13] B. Ghosh, V. K. Dwivedi, and S. Mukhopadhyay, *Phys. Rev. B* **102**, 144444 (2020).
- [14] A. Juyal, A. Agarwal, and S. Mukhopadhyay, *Phys. Rev. B* **95**, 125436 (2017).
- [15] A. Juyal, A. Agarwal, and S. Mukhopadhyay, *Phys. Rev. Lett.* **120**, 096801 (2018).
- [16] Z. Wang and S.-C. Zhang, *Phys. Rev. B* **87**, 161107(R) (2013).
- [17] J. Gooth, B. Bradlyn, S. Honnali *et al.*, *Nature (London)* **575**, 315 (2019).
- [18] M. Nakayama, T. Kondo, Z. Tian, J. J. Ishikawa, M. Halim, C. Bareille, W. Malaeb, K. Kuroda, T. Tomita, S. Ideta, K. Tanaka, M. Matsunami, S. Kimura, N. Inami, K. Ono, H. Kumigashira, L. Balents, S. Nakatsuji, and S. Shin, *Phys. Rev. Lett.* **117**, 056403 (2016).
- [19] A. B. Sushkov, J. B. Hofmann, G. S. Jenkins, J. Ishikawa, S. Nakatsuji, S. Das Sarma, and H. D. Drew, *Phys. Rev. B* **92**, 241108(R) (2015).
- [20] Y. Li, T. Oh, J. Son, J. Song, M. Kyung Kim, D. Song, S. Kim, S. H. Chang, C. Kim, B.-J. Yang, and T. Won Noh, *Adv. Mater.* **33**, 2008528 (2021).
- [21] P. Hosur, S. A. Parameswaran, and A. Vishwanath, *Phys. Rev. Lett.* **108**, 046602 (2012).
- [22] See Supplemental Material at <http://link.aps.org/supplemental/10.1103/PhysRevB.106.155149> for additional details about (i) sample preparation and characterization, (ii) negative longitudinal and positive transverse MR in bulk polycrystalline $\text{Y}_2\text{Ir}_2\text{O}_7$, (iii) ac response of the WSM and the CDW phase in $\text{Y}_2\text{Ir}_2\text{O}_7$, (iv) the ac conductivity of disordered WSM.
- [23] S. M. Dubiel and J. Cieslak, *Phys. Rev. B* **51**, 9341 (1995).
- [24] J. Bardeen, *Phys. Rev. Lett.* **45**, 1978 (1980).
- [25] K. Maki, *Phys. Rev. B* **33**, 2852(R) (1986); K. Maki and A. Virosztek, *ibid.* **39**, 9640 (1989); **42**, 655 (1990); X. Huang and K. Maki, *ibid.* **42**, 6498 (1990).
- [26] G. Grüner, *Rev. Mod. Phys.* **60**, 1129 (1988).
- [27] G. Gruner, *Density Waves in Solids* (Perseus Publishing, Cambridge, 2000).
- [28] P. Monceau, J. Richard, and M. Renard, *Phys. Rev. B* **25**, 931 (1982).
- [29] G. Blumberg, P. Littlewood, A. Gozar, B. S. Dennis, N. Motoyama, H. Eisaki, and S. Uchida, *Science* **297**, 584 (2002).
- [30] J. R. Tucker, W. G. Lyons, J. H. Miller, Jr., R. E. Thorne, and J. W. Lyding, *Phys. Rev. B* **34**, 9038(R) (1986).
- [31] M. Yao, W. Liud, X. Chena, Z. Renb, S. Wilsonc, Z. Renb, and C. P. Opeila, *J. Materiomics* **3**, 150 (2017).

- [32] H. Kumar, R. S. Dhaka, and A. K. Pramanik, *Phys. Rev. B* **95**, 054415 (2017).
- [33] P. G. LaBarre, L. Dong, J. Trinh, T. Siegrist, and A. P. Ramirez, *J. Phys.: Condens. Matter* **32**, 02LT01 (2020).
- [34] S. M. Disseler, C. Dhital, A. Amato, S. R. Giblin, C. de la Cruz, S. D. Wilson, and M. J. Graf, *Phys. Rev. B* **86**, 014428 (2012).
- [35] H. Liu, W. Tong, L. Ling, S. Zhang, R. Zhang, L. Zhang, L. Pi, C. Zhang, and Y. Zhang, *Solid State Commun.* **179**, 1 (2014).
- [36] C. R. Rajamathi *et al.*, *Adv. Mater.* **29**, 1606202 (2017).
- [37] Q.-G. Mu, D. Nenno, Y.-P. Qi, F.-R. Fan, C. Pei, M. ElGhazal, J. Gooth, C. Felser, P. Narang, and S. Medvedev, *Phys. Rev. Mater.* **5**, 084201 (2021).
- [38] V. Eremenko, V. Sirenko, V. Ibulaev, J. Bartolomé, A. Arauzo, and G. Reményi, *Physica C* **469**, 259 (2009).
- [39] N. Taira, M. Wakeshima, and Y. Hinatsu, *J. Phys.: Condens. Matter* **13**, 5527 (2001).
- [40] K. Biljakovic, J. C. Lasjaunias, F. Zougmore, P. Monceau, F. Levy, L. Bernard, and R. Currat, *Phys. Rev. Lett.* **57**, 1907 (1986).
- [41] A. Cano and A. P. Levanyuk, *Phys. Rev. Lett.* **93**, 245902 (2004).
- [42] G. Remenyi, S. Sahling, K. Biljakovic, D. Staresinic, J.-C. Lasjaunias, J. E. Lorenzo, P. Monceau, and A. Cano, *Phys. Rev. Lett.* **114**, 195502 (2015).